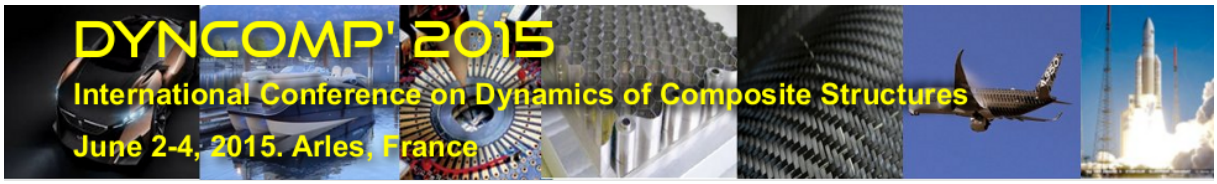

A MIXED "BIOT-SHELL" ANALYTICAL MODEL FOR THE CALCULATION OF SOUND TRANSMISSION THROUGH SANDWICH CYLINDERS WITH POROELASTIC CORES

Julien Magniez[1*] , Mohamed Ali Hamdi[1] , Jean-Daniel Chazot[1] and Bernard Troclet[2]

[1]Laboratoire Roberval UMR 7337
Université de Technologie de Compiègne, CS 60319, 60203 Compiègne cedex, FRANCE
Email: julien.magniez@utc.fr, mohamed-ali.hamdi@utc.fr, jean-daniel.chazot@utc.fr

[2]Airbus Defence & Space
51-61 Route de Verneuil, BP 3002, 78133 Les Mureaux Cedex, FRANCE
Email: bernard.troclet@astrium.eads.net

ABSTRACT

In this work, the sound transmission through a sandwich cylinder with a poroelastic core is studied analytically. The cylinder is composed of two orthotropic skins, modeled with a shell theory, and a poroelastic core modeled with the full 3D Biot's theory. Thus, a mixed "Biot-Shell" analytical model is presented in this paper. First, the motion of the sandwich cylinder obtained with this mixed "Biot-Shell" model is presented. Then, the model is used to calculate the sound transmission in the case of an excitation by an external oblique plane wave. A very good agreement is found when the results are compared to those obtained with a finite element model. Finally, some results are presented and the Transmission Loss (TL) is studied in different configurations. The main conclusion obtained from the results is that the poroelastic coating can significantly improve the TL of a cylindrical structure in mid- and high frequencies.

1 INTRODUCTION

Multilayer cylinders are widely used in aeronautics and aerospace industries. Generally designed to be as light as possible, these structures must also take into account the problem of inner noise transmission. Indeed, protection against noise is still necessary in such applications, whether it is for the passengers comfort or the payload protection. Thus, an optimization tool is necessary to reduce the total weight of the structure while increasing its acoustic efficiency. Consequently, fast analytical models have to be developed in order to predict accurately the sound transmission through these cylindrical structures.

In these applications, poroelastic materials are commonly used to reduce significantly the noise transmitted inside the compartment. Many studies have been made to model the behavior of these porous materials, and literature reveals a large number of publications on this subject. However, the state of the art shows that there are two main approaches to model them. The first way is to model them as equivalent fluids [1]. In these models, the viscous and thermal effects due to the skeleton are considered, but the skeleton elasticity is neglected. The second way is to use Biot's model [2, 3]. In the case of Biot's model, the motion of the skeleton is taken into account through the elastodynamic equations. This basic model considers the porous material as a superposition of two coupled solid and fluid phases. It is more adapted to model the dynamic behavior of poroelastic materials.

In this paper, the sound transmission through a sandwich cylinder having a poroelastic core modeled with Biot's theory is studied analytically. The two skins of the sandwich structure are orthotropic and modeled with a shell model. Thus, a mixed "Biot-Shell" analytical model is presented in this paper. In section 2, the motion of the sandwich cylinder obtained with this mixed "Biot-Shell" model is presented. The transfer matrix of the poroelastic core is used to couple the two skins. In section 3, the model is used to calculate the sound transmission when the cylinder is excited by an external oblique plane wave. In section 4, numerical results obtained with the proposed model are presented. As firstly shown, a very good agreement is found when the results are compared to those obtained with a finite element model. Then, the Transmission Loss (TL) is studied in different configurations. Finally, the main conclusions are presented in section 5.

2 VIBRATIONS OF THE SANDWICH CYLINDER

The sandwich structure and the notations used in the following are presented in detail in Figure 1. Note that layers 1 and 3 refer to the inner and outer skins respectively, and that layer 2 designates the poroelastic core.

2.1 Motion of the orthotropic skins

For each skin i ($i = 1, 3$) the displacement field is given by the First-order Shear Deformation Theory (FSDT):

$$u^i(z,\theta,\xi) = u_0^i(z,\theta) + \xi\psi_z^i(z,\theta), \tag{1a}$$

$$v^i(z,\theta,\xi) = v_0^i(z,\theta) + \xi\psi_\theta^i(z,\theta), \tag{1b}$$

$$w^i(z,\theta,\xi) = w_0^i(z,\theta), \tag{1c}$$

where u_0^i, v_0^i and w_0^i are the displacements at $\xi = 0$ of the layer i in the axial, circumferential and radial directions, respectively, and ψ_z^i and ψ_θ^i are the rotations of the normal to the median surface of each layer i. Note that the ξ-axis origin is at the median surface of the cylinder (see Figure 1).

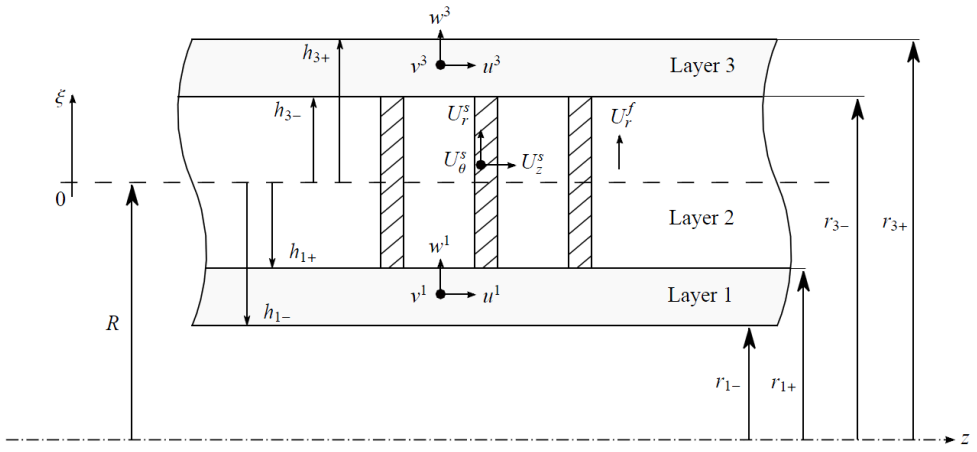

Figure 1. Sandwich structure and notations.

For each skin, five equilibrium equations are written in terms of displacements as (see [4, 5] for more details):

$$\mathbf{L}^i\mathbf{u}^i + \mathbf{M}^i\ddot{\mathbf{u}}^i = \mathbf{q}^i, \tag{2}$$

with $\mathbf{u}^i$ the displacement-rotation vector and $\mathbf{q}^i$ the force-moment vector given by:

$$\mathbf{u}^i = \left[u_0^i, v_0^i, w_0^i, \psi_z^i, \psi_\theta^i\right]^T \quad \text{and} \quad \mathbf{q}^i = \left[q_z^i, q_\theta^i, q_r^i, m_z^i, m_\theta^i\right]^T. \tag{3}$$

Moreover, $\mathbf{L}^i$ is the stiffness operator and $\mathbf{M}^i$ is the mass matrix, which are not given here for sake of conciseness but can be found in reference [5].

2.2 Transfer matrix of the poroelastic core

Biot's theory is used to describe the motion of the poroelastic core. The classical Biot's equations involve the solid phase (skeleton) displacement field $\mathbf{U}^s$ and the fluid phase displacement field $\mathbf{U}^f$ [1, 2]. However, it has been shown by Atalla *et al.* [6] that Biot's equations can be rewritten in order to introduce the interstitial pressure p instead of the fluid displacement field $\mathbf{U}^f$. This mixed $(\mathbf{U}^s, p)$ formulation has the great advantage of reducing the number of degrees of freedom per node from 6 to 4 in a finite element implementation. Moreover, according to Hamdi *et al.* [7], the mixed formulation presented by Atalla *et al.* [6] can be reformulated in order to involve explicitly the total stress tensor in the poroelastic medium. In this way, the associated weak integral formulation has the great advantage of leading to natural coupling conditions at the interface between two adjacent layers [7, 8]. The combination between the method given by Atalla *et al.* [6] and the formulation proposed by Hamdi *et al.* [7] leads to the following mixed Biot's equations, written in terms of the solid phase displacement field $\mathbf{U}^s$ and the interstitial pressure p:

$$\tilde{\rho}\omega^2\mathbf{U}^s + \nabla\cdot(\hat{\boldsymbol{\sigma}}^s - \alpha\phi p\mathbf{I}) + \beta\nabla(\phi p) = 0, \tag{4}$$

$$\nabla\cdot\left(\frac{1}{\tilde{\rho}_{22}\omega^2}\nabla(\phi p) - \beta\mathbf{U}^s\right) + \frac{\phi p}{\tilde{R}} + \alpha\nabla\cdot\mathbf{U}^s = 0, \tag{5}$$

where ϕ is the porosity, $\hat{\boldsymbol{\sigma}}^s$ the stress tensor of the skeleton *in vacuo*, and $\mathbf{I}$ the identity matrix. The terms $\alpha = 1 + \frac{\tilde{Q}}{\tilde{R}}$ and $\beta = 1 + \frac{\tilde{\rho}_{12}}{\tilde{\rho}_{22}}$ are two coupling factors between the skeleton and the interstitial fluid. Moreover, the effective densities $\tilde{\rho}$, $\tilde{\rho}_{12}$, and $\tilde{\rho}_{22}$ and the elastic coefficients $\tilde{Q}$ and $\tilde{R}$ can be found in reference [1]. Note however that the time convention $\mathrm{e}^{-\mathrm{j}\omega t}$ is taken here with an angular frequency ω.

By using the stress-displacement relation $\hat{\boldsymbol{\sigma}}^s = \lambda\left(\nabla\cdot\mathbf{U}^s\right)\mathbf{I} + \mu\left(\nabla\mathbf{U}^s + (\nabla\mathbf{U}^s)^T\right)$, the first mixed Biot's equation (4) becomes:

$$\tilde{\rho}\omega^2\mathbf{U}^s + (\lambda+2\mu)\nabla(\nabla\cdot\mathbf{U}^s) - \tilde{\gamma}\nabla(\phi p) - \mu\nabla\wedge\nabla\wedge\mathbf{U}^s = 0, \tag{6}$$

where λ and μ are the Lamé coefficient of the skeleton *in vacuo* and $\tilde{\gamma} = \alpha - \beta$. To solve this equation, the following Helmholtz decomposition is used for the solid displacement:

$$\mathbf{U}^s = \nabla\left(\varphi_1^s + \varphi_2^s\right) + \nabla\wedge\boldsymbol{\psi}^s, \tag{7}$$

where φ_1^s and φ_2^s are the scalar potentials related to the two longitudinal waves, and $\boldsymbol{\psi}^s$ the vector potential related to the shear wave in the poroelastic medium. Substituting the decomposition (7) into Biot's equations (6) and (5) gives, all calculations done, three wave equations fulfilled by each of the potentials:

$$\Delta\varphi_1^s + \frac{\omega^2}{c_1^2}\varphi_1^s = 0, \quad \Delta\varphi_2^s + \frac{\omega^2}{c_2^2}\varphi_2^s = 0 \quad \text{and} \quad \Delta\boldsymbol{\psi}^s + \frac{\omega^2}{c_3^2}\boldsymbol{\psi}^s = 0, \tag{8}$$

where Δ is the Laplacian operator, c_1 and c_2 the celerity of the two longitudinal waves and c_3 the celerity of the shear wave. The details of c_1, c_2 and c_3 can be found in reference [1]. The substitution of (7) into (6) also gives a relation between the interstitial pressure and the scalar potentials:

$$p = \frac{1}{\tilde{\gamma}\phi}\left((\lambda+2\mu)\Delta\left(\varphi_1^s + \varphi_2^s\right) + \tilde{\rho}\omega^2\left(\varphi_1^s + \varphi_2^s\right)\right). \tag{9}$$

The general solutions of the wave equations given in (8) are expanded in cylindrical harmonics. By substituting these solutions into equation (7), the following solid displacement field is obtained:

$$U_r^s(r,\theta,z,t) = \sum_{n=0}^{\infty} U_r^{s,n}(r)\cos(n\theta)\mathrm{e}^{\mathrm{j}k_z z - \mathrm{j}\omega t}, \tag{10a}$$

$$U_\theta^s(r,\theta,z,t) = \sum_{n=0}^{\infty} U_\theta^{s,n}(r)\sin(n\theta)\mathrm{e}^{\mathrm{j}k_z z - \mathrm{j}\omega t}, \tag{10b}$$

$$U_z^s(r,\theta,z,t) = \sum_{n=0}^{\infty} \mathrm{j}U_z^{s,n}(r)\cos(n\theta)\mathrm{e}^{\mathrm{j}k_z z - \mathrm{j}\omega t}, \tag{10c}$$

where n designates the circumferential order and k_z the axial wavenumber. Moreover, U_r^s, U_θ^s and U_z^s are the radial, circumferential and axial components respectively. The fluid displacement $\mathbf{U}^f$ is also related to the scalar and vector potentials with

$$\mathbf{U}^f = \nabla\left(\mu_1\varphi_1^s + \mu_2\varphi_2^s\right) + \nabla\wedge\mu_3\boldsymbol{\psi}^s, \tag{11}$$

where the amplitude ratios μ_1, μ_2 and μ_3 can be found in reference [1]. The radial component is thus also expanded in cylindrical harmonics as follows:

$$U_r^f(r,\theta,z,t) = \sum_{n=0}^{\infty} U_r^{f,n}(r)\cos(n\theta)\mathrm{e}^{\mathrm{j}k_z z - \mathrm{j}\omega t}. \tag{12}$$

The stress components are also needed to characterize the poroelastic medium. The total stress tensor in the poroelastic medium $\boldsymbol{\sigma}^t$ is the sum of a tensor related to the solid phase $\hat{\boldsymbol{\sigma}}^s$ and a tensor related to the fluid phase $\hat{\boldsymbol{\sigma}}^f$:

$$\boldsymbol{\sigma}^t = \hat{\boldsymbol{\sigma}}^s + \hat{\boldsymbol{\sigma}}^f, \tag{13}$$

where the notation $\hat{\boldsymbol{\sigma}}^f = -\alpha\phi p\mathbf{I}$ has been introduced. The solid phase stress tensor is obtained by using the stress-displacement relation. This yields:

$$\hat{\sigma}^s_{rr}(r,\theta,z,t) = \sum_{n=0}^{\infty} \hat{\sigma}^{s,n}_{rr}(r)\cos(n\theta)\mathrm{e}^{\mathrm{j}k_z z - \mathrm{j}\omega t}, \tag{14a}$$

$$\hat{\sigma}^s_{r\theta}(r,\theta,z,t) = \sum_{n=0}^{\infty} \hat{\sigma}^{s,n}_{r\theta}(r)\sin(n\theta)\mathrm{e}^{\mathrm{j}k_z z - \mathrm{j}\omega t}, \tag{14b}$$

$$\hat{\sigma}^s_{rz}(r,\theta,z,t) = \sum_{n=0}^{\infty} \mathrm{j}\hat{\sigma}^{s,n}_{rz}(r)\cos(n\theta)\mathrm{e}^{\mathrm{j}k_z z - \mathrm{j}\omega t}. \tag{14c}$$

The tensor $\hat{\boldsymbol{\sigma}}^f$ is obtained by using the expression of p given in equation (9). The scalar potentials φ^s_1 and φ^s_2 being defined in cylindrical coordinates, this tensor is also expanded in cylindrical harmonics. This yields for $\hat{\sigma}^f_{rr}$:

$$\hat{\sigma}^f_{rr}(r,\theta,z,t) = \sum_{n=0}^{\infty} \hat{\sigma}^{f,n}_{rr}(r)\cos(n\theta)\mathrm{e}^{\mathrm{j}k_z z - \mathrm{j}\omega t}. \tag{15}$$

The modal transfer matrix method is now used to relate the displacements and stresses at each interface of the poroelastic core. The modal amplitudes at the interfaces $r = r_{1+}$ and $r = r_{3-}$ of the core are hence related with:

$$\hat{\mathbf{S}}(r_{1+}) = \hat{\mathbf{T}}\hat{\mathbf{S}}(r_{3-}), \tag{16}$$

where $\hat{\mathbf{S}}(r) = \left[U^{s,n}_z(r), U^{s,n}_\theta(r), U^{s,n}_r(r), U^{f,n}_r(r), \hat{\sigma}^{s,n}_{rz}(r), \hat{\sigma}^{s,n}_{r\theta}(r), \hat{\sigma}^{s,n}_{rr}(r), \hat{\sigma}^{f,n}_{rr}(r)\right]^T$ is the modal amplitude vector, and $\hat{\mathbf{T}}$ is the 8×8 modal transfer matrix. Equation (16) can be rewritten in order to express the stresses components in terms of the displacements components. This yields:

$$\hat{\boldsymbol{\sigma}}^{1-3}_n = \hat{\mathbf{k}}\,\hat{\mathbf{U}}^{1-3}_n, \tag{17}$$

with

$$\hat{\boldsymbol{\sigma}}^{1-3}_n = \left[\hat{\sigma}^{s,n}_{rz}(r_{1+}), \hat{\sigma}^{s,n}_{r\theta}(r_{1+}), \hat{\sigma}^{s,n}_{rr}(r_{1+}), \hat{\sigma}^{f,n}_{rr}(r_{1+}), -\hat{\sigma}^{s,n}_{rz}(r_{3-}), -\hat{\sigma}^{s,n}_{r\theta}(r_{3-}), -\hat{\sigma}^{s,n}_{rr}(r_{3-}), -\hat{\sigma}^{f,n}_{rr}(r_{3-})\right]^T, \tag{18}$$

and

$$\hat{\mathbf{U}}^{1-3}_n = \left[U^{s,n}_z(r_{1+}), U^{s,n}_\theta(r_{1+}), U^{s,n}_r(r_{1+}), U^{f,n}_r(r_{1+}), U^{s,n}_z(r_{3-}), U^{s,n}_\theta(r_{3-}), U^{s,n}_r(r_{3-}), U^{f,n}_r(r_{3-})\right]^T. \tag{19}$$

The matrix $\hat{\mathbf{k}}$ is homogeneous to a stiffness matrix and is build from the components of the modal transfer matrix $\hat{\mathbf{T}}$.

2.3 Coupling conditions

(i) The continuity of the displacements must be satisfied at the core-skin interfaces. At $r = r_{1+}$ (interface between layers 1 and 2) this condition writes:

$$U^s_z(r_{1+},\theta,z) = u^1(z,\theta,h_{1+}) = u^1_0(z,\theta) + h_{1+}\psi^1_z(z,\theta), \tag{20a}$$

$$U^s_\theta(r_{1+},\theta,z) = v^1(z,\theta,h_{1+}) = v^1_0(z,\theta) + h_{1+}\psi^1_\theta(z,\theta), \tag{20b}$$

$$U^s_r(r_{1+},\theta,z) = w^1(z,\theta,h_{1+}) = w^1_0(z,\theta), \tag{20c}$$

$$U^f_r(r_{1+},\theta,z) = w^1(z,\theta,h_{1+}) = w^1_0(z,\theta), \tag{20d}$$

while at $r = r_{3-}$ (interface between layers 2 and 3) it writes:

$$U_z^s(r_{3-},\theta,z) = u^3(z,\theta,h_{3-}) = u_0^3(z,\theta) + h_{3-}\psi_z^3(z,\theta), \tag{21a}$$
$$U_\theta^s(r_{3-},\theta,z) = v^3(z,\theta,h_{3-}) = v_0^3(z,\theta) + h_{3-}\psi_\theta^3(z,\theta), \tag{21b}$$
$$U_r^s(r_{3-},\theta,z) = w^3(z,\theta,h_{3-}) = w_0^3(z,\theta), \tag{21c}$$
$$U_r^f(r_{3-},\theta,z) = w^3(z,\theta,h_{3-}) = w_0^3(z,\theta). \tag{21d}$$

(ii) Instead of using the stress continuity explicitly, the forces $\mathbf{q}^i$ appearing in the right-hand side of the skins equations (2) will be split as the sum of the generalized reaction forces $\hat{\mathbf{q}}^i_{core}$ applied by the poroelastic core on the skin i, and of the external forces $\mathbf{q}^i_{ext}$:

$$\mathbf{L}^i\mathbf{u}^i + \mathbf{M}^i\ddot{\mathbf{u}}^i = \hat{\mathbf{q}}^i_{core} + \mathbf{q}^i_{ext}. \tag{22}$$

The generalized core reaction forces given here are obtained by using the stress components of the poroelastic core in Eqs. (14) and (15) such as:

$$\hat{\mathbf{q}}^1_{core} = \begin{bmatrix} \hat{\sigma}^s_{rz}(r_{1+},\theta,z,t) \\ \hat{\sigma}^s_{r\theta}(r_{1+},\theta,z,t) \\ \hat{\sigma}^s_{rr}(r_{1+},\theta,z,t) + \hat{\sigma}^f_{rr}(r_{1+},\theta,z,t) \\ h_{1+}\hat{\sigma}^s_{rz}(r_{1+},\theta,z,t) \\ h_{1+}\hat{\sigma}^s_{r\theta}(r_{1+},\theta,z,t) \end{bmatrix} \text{ and } \hat{\mathbf{q}}^3_{core} = -\begin{bmatrix} \hat{\sigma}^s_{rz}(r_{3-},\theta,z,t) \\ \hat{\sigma}^s_{r\theta}(r_{3-},\theta,z,t) \\ \hat{\sigma}^s_{rr}(r_{3-},\theta,z,t) + \hat{\sigma}^f_{rr}(r_{3-},\theta,z,t) \\ h_{3-}\hat{\sigma}^s_{rz}(r_{3-},\theta,z,t) \\ h_{3-}\hat{\sigma}^s_{r\theta}(r_{3-},\theta,z,t) \end{bmatrix}. \tag{23}$$

and while the external forces $\mathbf{q}^i_{ext}$ write:

$$\mathbf{q}^i_{ext} = \left[f^i_{z,ext}, f^i_{\theta,ext}, f^i_{r,ext}, m^i_{z,ext}, m^i_{\theta,ext}\right]^T, \tag{24}$$

with $f^i_{z,ext}$, $f^i_{\theta,ext}$ and $f^i_{r,ext}$ the external forces per unit area, and $m^i_{z,ext}$ and $m^i_{\theta,ext}$ the external moments per unit area.

2.4 Global dynamic equilibrium

The two equations of motion of the skins are firstly grouped into a single system:

$$\begin{bmatrix} \mathbf{L}^1 & \mathbf{0} \\ \mathbf{0} & \mathbf{L}^3 \end{bmatrix}\begin{bmatrix} \mathbf{u}^1 \\ \mathbf{u}^3 \end{bmatrix} + \begin{bmatrix} \mathbf{M}^1 & \mathbf{0} \\ \mathbf{0} & \mathbf{M}^3 \end{bmatrix}\begin{bmatrix} \ddot{\mathbf{u}}^1 \\ \ddot{\mathbf{u}}^3 \end{bmatrix} = \begin{bmatrix} \hat{\mathbf{q}}^1_{core} \\ \hat{\mathbf{q}}^3_{core} \end{bmatrix} + \begin{bmatrix} \mathbf{q}^1_{ext} \\ \mathbf{q}^3_{ext} \end{bmatrix}, \tag{25}$$

and, as in section 2.2 for the core displacement, the skins displacements and the external forces are expanded in cylindrical harmonics:

$$\begin{bmatrix} u^i_0 \\ v^i_0 \\ w^i_0 \\ \psi^i_z \\ \psi^i_\theta \end{bmatrix} = \sum_{n=0}^{\infty}\begin{bmatrix} \mathrm{j}u^i_{0n}\cos(n\theta) \\ v^i_{0n}\sin(n\theta) \\ w^i_{0n}\cos(n\theta) \\ \mathrm{j}\psi^i_{zn}\cos(n\theta) \\ \psi^i_{\theta n}\sin(n\theta) \end{bmatrix} \mathrm{e}^{\mathrm{j}k_z z - \mathrm{j}\omega t} \text{ and } \begin{bmatrix} f^i_{z,ext} \\ f^i_{\theta,ext} \\ f^i_{r,ext} \\ m^i_{z,ext} \\ m^i_{\theta,ext} \end{bmatrix} = \sum_{n=0}^{\infty}\begin{bmatrix} \mathrm{j}f^i_{zn,ext}\cos(n\theta) \\ f^i_{\theta n,ext}\sin(n\theta) \\ f^i_{rn,ext}\cos(n\theta) \\ \mathrm{j}m^i_{zn,ext}\cos(n\theta) \\ m^i_{\theta n,ext}\sin(n\theta) \end{bmatrix} \mathrm{e}^{\mathrm{j}k_z z - \mathrm{j}\omega t}. \tag{26}$$

Using the expressions of the skins displacements and of the external forces given in equation (26), equation of motion (25) can be rewritten for each circumferential mode n as follows:

$$\begin{bmatrix} \mathbf{K}^1 & \mathbf{0} \\ \mathbf{0} & \mathbf{K}^3 \end{bmatrix}\begin{bmatrix} \mathbf{u}^1_n \\ \mathbf{u}^3_n \end{bmatrix} - \omega^2\begin{bmatrix} \mathbf{M}^1 & \mathbf{0} \\ \mathbf{0} & \mathbf{M}^3 \end{bmatrix}\begin{bmatrix} \mathbf{u}^1_n \\ \mathbf{u}^3_n \end{bmatrix} = \begin{bmatrix} \hat{\mathbf{q}}^1_{n,core} \\ \hat{\mathbf{q}}^3_{n,core} \end{bmatrix} + \begin{bmatrix} \mathbf{q}^1_{n,ext} \\ \mathbf{q}^3_{n,ext} \end{bmatrix}, \tag{27}$$

where $\mathbf{u}_n^i$ is the displacement-rotation amplitude vector:

$$\mathbf{u}_n^i = \left[u_{0n}^i, v_{0n}^i, w_{0n}^i, \psi_{zn}^i, \psi_{\theta n}^i\right]^T, \tag{28}$$

$\hat{\mathbf{q}}_{n,core}^i$ is the generalized reaction amplitude vector:

$$\hat{\mathbf{q}}_{n,core}^1 = \begin{bmatrix} \hat{\sigma}_{rz}^{s,n}(r_{1+}) \\ \hat{\sigma}_{r\theta}^{s,n}(r_{1+}) \\ \hat{\sigma}_{rr}^{s,n}(r_{1+}) + \hat{\sigma}_{rr}^{f,n}(r_{1+}) \\ h_{1+}\hat{\sigma}_{rz}^{s,n}(r_{1+}) \\ h_{1+}\hat{\sigma}_{r\theta}^{s,n}(r_{1+}) \end{bmatrix} \quad \text{and} \quad \hat{\mathbf{q}}_{n,core}^3 = - \begin{bmatrix} \hat{\sigma}_{rz}^{s,n}(r_{3-}) \\ \hat{\sigma}_{r\theta}^{s,n}(r_{3-}) \\ \hat{\sigma}_{rr}^{s,n}(r_{3-}) + \hat{\sigma}_{rr}^{f,n}(r_{3-}) \\ h_{3-}\hat{\sigma}_{rz}^{s,n}(r_{3-}) \\ h_{3-}\hat{\sigma}_{r\theta}^{s,n}(r_{3-}) \end{bmatrix}, \tag{29}$$

$\mathbf{q}_{n,ext}^i$ is the external force amplitude vector:

$$\mathbf{q}_{n,ext}^i = \left[f_{zn,ext}^i, f_{\theta n,ext}^i, f_{rn,ext}^i, m_{zn,ext}^i, m_{\theta n,ext}^i\right]^T, \tag{30}$$

and $\mathbf{K}^i$ is the stiffness matrix given in reference [5].

The generalized reaction amplitude vectors $\hat{\mathbf{q}}_{n,core}^1$ and $\hat{\mathbf{q}}_{n,core}^3$ appearing in the right-hand side of Eq. (27) can be written in terms of the skins displacements, using equations (17), (20) and (21). The resulting generalized reaction amplitude vectors write hence:

$$\begin{bmatrix} \hat{\mathbf{q}}_{n,core}^1 \\ \hat{\mathbf{q}}_{n,core}^3 \end{bmatrix} = \begin{bmatrix} \hat{\mathbf{K}}_{11}^2 & \hat{\mathbf{K}}_{13}^2 \\ \hat{\mathbf{K}}_{31}^2 & \hat{\mathbf{K}}_{33}^2 \end{bmatrix} \begin{bmatrix} \mathbf{u}_n^1 \\ \mathbf{u}_n^3 \end{bmatrix}, \tag{31}$$

and after substitution of this equation in (27), we finally obtain:

$$\begin{bmatrix} \mathbf{K}^1 - \hat{\mathbf{K}}_{11}^2 & -\hat{\mathbf{K}}_{13}^2 \\ -\hat{\mathbf{K}}_{31}^2 & \mathbf{K}^3 - \hat{\mathbf{K}}_{33}^2 \end{bmatrix} \begin{bmatrix} \mathbf{u}_n^1 \\ \mathbf{u}_n^3 \end{bmatrix} - \omega^2 \begin{bmatrix} \mathbf{M}^1 & \mathbf{0} \\ \mathbf{0} & \mathbf{M}^3 \end{bmatrix} \begin{bmatrix} \mathbf{u}_n^1 \\ \mathbf{u}_n^3 \end{bmatrix} = \begin{bmatrix} \mathbf{q}_{n,ext}^1 \\ \mathbf{q}_{n,ext}^3 \end{bmatrix}. \tag{32}$$

Equation (32) describes the motion of the entire structure excited by external forces. This equation clearly shows the coupling between the inner and the outer skin with the impedance matrix of the poroelastic core $\hat{\mathbf{K}}^2(\omega)$.

3 VIBROACOUSTIC PROBLEM

3.1 Global vibroacoustic system

In this paper, the cylinder is excited by an external oblique plane wave. For this kind of excitation, the external forces acting on the structure are the following:

$$\mathbf{q}_{ext}^1 = [0, 0, p_2(r_{1-}, \theta, z, t), 0, 0]^T \quad \text{and} \quad \mathbf{q}_{ext}^3 = [0, 0, -p_1(r_{3+}, \theta, z, t), 0, 0]^T, \tag{33}$$

where p_1 and p_2 are the acoustic pressures in the external medium and in the cavity respectively. In reference [5] it is shown that for this kind of excitation, the external force amplitude vectors $\mathbf{q}_{n,ext}^i$ can be written in terms of the skins displacement amplitude vectors $\mathbf{u}_n^i$ in the following form:

$$\begin{bmatrix} \mathbf{q}_{n,ext}^1 \\ \mathbf{q}_{n,ext}^3 \end{bmatrix} = \begin{bmatrix} \mathbf{Z}^1 & \mathbf{0} \\ \mathbf{0} & \mathbf{Z}^3 \end{bmatrix} \begin{bmatrix} \mathbf{u}_n^1 \\ \mathbf{u}_n^3 \end{bmatrix} + \begin{bmatrix} \mathbf{0} \\ \mathbf{p}_n^b \end{bmatrix}, \tag{34}$$

where $\mathbf{p}_n^b$ is the blocked-wall vector expressed in terms of the blocked-wall pressure p^b. Moreover, $\mathbf{Z}^1$ and $\mathbf{Z}^3$ are impedance matrices expressed in terms of Z_{1n} and Z_{2n}, the radiation impedance of the external and internal surfaces of the cylinder respectively. The expressions of $\mathbf{p}_n^b$, $\mathbf{Z}^1$ and $\mathbf{Z}^3$ are given in reference [5]. Finally, the global vibroacoustic system is obtained by substituting (34) into (32):

$$\begin{bmatrix} \mathbf{K}^1 - \hat{\mathbf{K}}_{11}^2 - \mathbf{Z}^1 & -\hat{\mathbf{K}}_{13}^2 \\ -\hat{\mathbf{K}}_{31}^2 & \mathbf{K}^3 - \hat{\mathbf{K}}_{33}^2 - \mathbf{Z}^3 \end{bmatrix} \begin{bmatrix} \mathbf{u}_n^1 \\ \mathbf{u}_n^3 \end{bmatrix} - \omega^2 \begin{bmatrix} \mathbf{M}^1 & \mathbf{0} \\ \mathbf{0} & \mathbf{M}^3 \end{bmatrix} \begin{bmatrix} \mathbf{u}_n^1 \\ \mathbf{u}_n^3 \end{bmatrix} = \begin{bmatrix} \mathbf{0} \\ \mathbf{p}_n^b \end{bmatrix}. \tag{35}$$

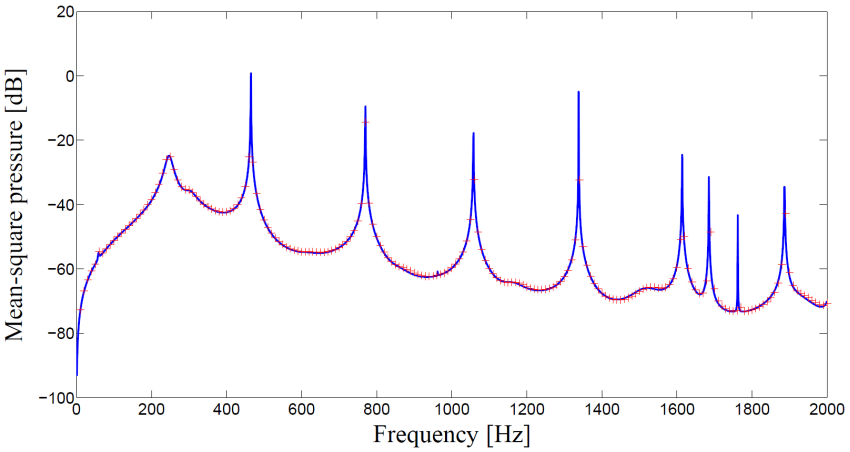

Figure 2: Comparison of the mean-square pressure obtained with the present mixed "Biot-Shell" analytical model and with a finite element model for a sandwich cylinder excited by a plane wave ($\gamma = 0°$). (—) Mixed "Biot-Shell" analytical model, (+) finite element model.

3.2 Transmission Loss calculation

The Transmission Loss (TL) is used to characterize the sound transmission. The TL is defined by:

$$TL = 10 \log \frac{W^I}{W^T}, \tag{36}$$

where W^I and W^T are the incident and transmitted powers, respectively. All calculations done, the TL is found in the following form (see reference [5] for more details):

$$TL = -10 \log \sum_{n=0}^{\infty} \frac{\text{Re}\left\{Z_{2n} w_{0n}^1 \cdot (-\text{j}\omega w_{0n}^1)^*\right\} r_{1-} \rho_1 c_{01} \pi}{r_{3+} p_0^2 \varepsilon_n \cos\gamma}, \tag{37}$$

where γ is the incidence angle with respect to the normal of the cylinder. Moreover, p_0 is the amplitude of the incident wave, ε_n is the Neumann factor ($\varepsilon_n = 1$ if $n = 0$, $\varepsilon_n = 2$ if $n \neq 0$), ρ_1 and c_{01} are the density and the speed of sound in the external fluid, and Re$\{.\}$ and $*$ are the real part and the complex conjugate, respectively. The displacement amplitude w_{0n}^1 is obtained by solving the global vibroacoustic system (35) for each circumferential mode n.

4 RESULTS

4.1 Analytical model validation

In this section, the mixed "Biot-Shell" analytical model is validated with a finite element model. The problem studied here is the acoustic transmission through an infinite cylinder. To simulate the axially infinite extent, a 2-dimensional finite element model in the (r-θ) plane is used, and the external plane wave is applied at normal incidence with respect to the cylinder axis ($\gamma = 0°$). The model is meshed with linear triangular elements, and an absorbent Perfectly Matched Layer (PML) is also used to impose a non-reflection boundary condition. Note that a resonant cavity is considered in the finite element model. This condition is therefore also applied in the analytical model. Finally, the mean-square pressure $\langle p_{int}^2 \rangle$ in the internal cylindrical cavity is used herein to compare the two methods.

Figure 2 presents the mean-square pressure obtained with the two methods, in the case of a sandwich cylinder having aluminum skins of 5 mm and a foam core of 20 mm, whose properties are given in reference [9]. A very good agreement is obtained between the mixed

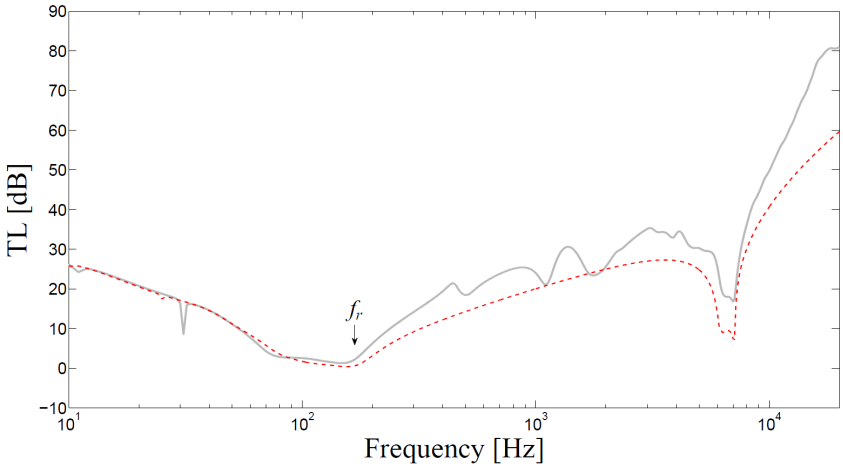

Figure 3: Effect of the poroelastic material on the TL of a cylinder excited by a plane wave ($\gamma = 45°$). (- -) Single shell, (—) shell + poroelastic coating (two-layer configuration).

"Biot-Shell" analytical model and the finite element model. Other configurations have also been tested and have given similar results. The analytical model is hence validated. Note also that the computation time of the analytical model is very low compared to the finite element model.

4.2 Poroelastic material effects

The mixed "Biot-Shell" analytical model is now used to study the influence of the poroelastic material on sound transmission. To do this, two configurations are studied. The first one is the single shell configuration, where a single orthotropic shell is considered. The second one is the two-layer configuration, where a poroelastic coating is added to the shell used in the first configuration. The orthotropic shell being the same in both cases, this allows us to directly study the influence of the poroelastic material on sound transmission. Note that the calculation is made for an aerospace configuration ($r_{3+} = 2.164$ m, shell thickness of 2 mm and poroelastic thickness of 50 mm). The results are presented in Figure 3.

In view of this figure, the ring frequency f_r separates two domains. Below the ring frequency, in very low frequencies ($f < 60$ Hz), adding a poroelastic material does not reduce sound transmission and the TL is not improved. Indeed, for $f < f_r$, the structure vibrates with a global behavior and sound transmission is primarily governed by the rigid shell. Nevertheless, the poroelastic layer shifts the frequencies of the structural resonances. However, it is found that around the ring frequency, adding a poroelastic layer improves the TL. Indeed, a gain from 1 to 2 dB is observed in this frequency zone. This interesting result is explained by the fact that the poroelastic layer adds damping to the structure, which is mainly due to the thermal and viscous dissipation. Since the TL is dependent of the damping at the ring frequency, this explains why the results are improved with the poroelastic layer.

Observing now the results above the ring frequency, we see that the TL is significantly improved with the poroelastic material. Three factors can explain this phenomenon. First, the poroelastic material adds weight to the structure. This allows the TL to be increased, mainly in the mass-controlled zone (between 175 Hz and 6000 Hz). Then, the poroelastic material adds damping to the structure. Thus, it reduces the TL at its dips (between 6000 Hz and 7500 Hz in particular). Last but not least, the poroelastic material has a high power of absorption of acoustic waves, and its efficiency is greater when the frequency increases. This explains the improving of the TL in the mid- and high frequencies with the poroelastic coating.

Finally, since the mass of the poroelastic layer is low, adding this type of material is a very interesting solution to reduce the sound transmission through cylindrical structures.

5 CONCLUSION

In this paper, a mixed "Biot-Shell" analytical model has been presented. Its main advantage is to allow fast analytical calculations of sound transmission through orthotropic shells having a poroelastic coating, taking into account the elasticity effects of the poroelastic material.

Two important effects of the poroelastic layer were highlighted from the results obtained with the proposed model. The first one is to reduce significantly the sound transmission above the ring frequency, and the second one is to reduce the transmission around the ring frequency. The mass added by a poroelastic material being quite low, this is a very interesting solution to reduce sound transmission through a cylindrical structure.

In conclusion, the mixed "Biot-Shell" analytical model proposed in this paper is very well adapted to describe the behavior of an orthotropic cylinder having a poroelastic coating, since all the physical phenomena are taken into account in the poroelastic layer with Biot's model.

REFERENCES

[1] J.-F. Allard and N. Atalla. *Propagation of sound in porous media: modelling sound absorbing materials, second edition*. Wiley, 2009.

[2] M. A. Biot. Theory of propagation of elastic waves in a fluid-saturated porous solid. I. Low-frequency range. *J. Acoust. Soc. Am.*, 28(2):168–178, 1956.

[3] M. A. Biot. Theory of propagation of elastic waves in a fluid-saturated porous solid. II. Higher frequency range. *J. Acoust. Soc. Am.*, 28(2):179–191, 1956.

[4] M. S. Qatu. *Vibration of laminated shells and plates*. Elsevier Academic Press, Oxford, 2004.

[5] J. Magniez, J.-D. Chazot, M. A. Hamdi, and B. Troclet. A mixed 3D-Shell analytical model for the prediction of sound transmission through sandwich cylinders. *J. Sound Vib.*, 333(19):4750–4770, 2014.

[6] N. Atalla, R. Panneton, and P. Debergue. A mixed displacement-pressure formulation for poroelastic materials. *J. Acoust. Soc. Am.*, 104(3):1444–1452, 1998.

[7] M. A. Hamdi, L. Mebarek, A. Omrani, and N. Atalla. An efficient formulation for the analysis of acoustic and elastic waves propagation in porous-elastic materials. In *Proceedings of ISMA* 25*, International Conference on Noise and Vibration Engineering*, 2000.

[8] N. Atalla, M. A. Hamdi, and R. Panneton. Enhanced weak integral formulation for the mixed (u, p) poroelastic equations. *J. Acoust. Soc. Am.*, 109(6):3065–3068, 2001.

[9] J. Kanfoud, M. A. Hamdi, F.-X. Becot, and L. Jaouen. Development of an analytical solution of modified Biot's equations for the optimization of lightweight acoustic protection. *J. Acoust. Soc. Am.*, 125(2):863–872, 2009.